Journal of Solid State Chemistry 318 (2023) 123781

Contents lists available at ScienceDirect

Journal of Solid State Chemistry

journal homepage: www.elsevier.com/locate/jssc

Strong hydrogen bond in the crystal structure design of $CuNbOF_5{\cdot}4H_2O$

N.M. Laptash [a,*], A.A. Udovenko [a], A.D. Vasiliev [b], E.B. Merkulov [a]

[a] Institute of Chemistry, Far Eastern Branch of RAS, 159 Pr. Stoletiya Vladivostoka, 690022, Vladivostok, Russia
[b] Kirensky Institute of Physics, Siberian Branch of RAS, Academgorodok, 660036, Krasnoyarsk, Russia

ARTICLE INFO

Keywords:
Mixed transition metal oxyfluoride
Crystal structure
Strong hydrogen bond
Phase transition
Thermal analysis

ABSTRACT

Fluoride metal-organic frameworks (MOFs) based on pillared $[NbOF_5]^{2-}$ anion have been recently received research attention as ultramicroporous materials for gas storage and separation. The *trans*-directing property of the $NbOF_5$ octahedron plays a significant role in designing mixed metal oxyfluoride compounds composed of the alternating transition metal polyhedra, which are linked via oxide and fluoride ligands. Mixed metal $CuNbOF_5{\cdot}4H_2O$ is the only unique example when the *trans*-directing properties of $[NbOF_5]^{2-}$ are realized in the formation of a strong O–H···F hydrogen bond (HB). Well-shaped single crystals of this compound were grown and their structure was refined by X-ray diffraction. Under quasi-isobaric conditions, a phase transition at 88 °C takes place, which is associated with the weakening of HBs and formation of ordinary chains through conventional *trans*-(O,F) bridges. The character of hydrogen bonding in $CuNbOF_5{\cdot}4H_2O$ affects its thermal behavior described by the dehydration and pyrohydrolysis processes.

1. Introduction

Basic building units (BBUs) with individual net dipole moments are extensively used in solid-state chemistry for the engineering of new non-centrosymmetric materials with interesting physical properties, including piezoelectricity, ferroelectricity, nonlinear optical activity, and/or pyroelectricity. Key constituents for the engineering of polarity in oxyfluoride chemistry are early transition-metal (ETM)-centered anions with the formula $[MO_xF_{6-x}]^{2-}$ (x = 1, M = V, Nb, and Ta; x = 2, M = Mo and W) exhibiting out-of-center distortion. The combination of a late transition-metal (LTM) cation with an ETM anion $[MO_xF_{6-x}]^{2-}$ leads to mixed metal infinite chains. The alignment of polar units in infinite chains was described with a "lock and key" model, where the key was the acentric unit and the lock was its environment [1]. The out-of-center distortion of the ETMs in $[MO_xF_{6-x}]^{2-}$ anions is induced by the electronic effects, such as dπ–pπ metal oxide orbital interactions (primary distortion) and the interaction between the $[MO_xF_{6-x}]^{2-}$ anion and its environment (secondary distortion) [2]. For anions of the type $[MOF_5]^{2-}$ (M = Nb, Ta), the central metal distorts toward the single oxide, and a short apical M − O bond and a long *trans* M − F bond are observed in the crystal structure. This distortion leaves an unequal amount of residual negative charge on each ligand. In the $[NbOF_5]^{2-}$ anion, the significant charge density localizes on the oxide ion, and the fluoride ion *trans* to the oxide exhibits a higher electrostatic potential than the other four fluoride ions [3,4]. For this reason, $[NbOF_5]^{2-}$ is *trans*-directing anion because it directs the coordination through the nucleophilic oxide and its *trans*-fluoride. This structure-directing property of it can be used to control on the design of oxyfluoride materials. The combination of $[NbOF_5]^{2-}$ anionic units with *trans*-coordinating cationic units (LTM) results in a *trans–trans* linear or zigzag one-dimensional chain structure or in cluster compounds with oxygen or oxygen/fluorine bridges in most cases (see Table S1 in the Supporting Information). The crystal structural data of mixed metal-niobium compounds refer mainly to hybrid organic-inorganic complexes.

Metal-organic frameworks (MOFs) based on the pillared $[NbOF_5]^{2-}$ anion have been recently received research attention as ultramicroporous materials in the field of gas storage and separation, as noted in a series of very recent reviews [5–8]. Fluorinated MOF $NiNbOF_5(pyr)_2{\cdot}2H_2O$, pyr = pyrazine (NbOFFIVE-1-Ni, also known as KAUST-7) synthesized by Eddaoudi et al. has effectively been used for selective adsorption of C_3H_6 (propylene) with the complete exclusion of C_3H_8 (propane) [9,10]. This NbOFFIVE-1-Ni was also reported to be ideal for the effective and energy-efficient traces carbon dioxide removal and stands as the best physical-adsorbent material for CO_2 capture from atmospheric and confined spaces [11]. KAUST-7 was expected to be a new membrane material candidate for H_2/CO_2 separation because of the hindered permeation of CO_2 resulting from the interaction between CO_2 and $[NbOF_5]^{2-}$ of the KAUST-7 framework [12]. The NbOFFIVE-1-Ni

* Corresponding author.
E-mail address: laptash@ich.dvo.ru (N.M. Laptash).

https://doi.org/10.1016/j.jssc.2022.123781
Received 27 September 2022; Received in revised form 30 November 2022; Accepted 5 December 2022
Available online 6 December 2022

MOF was also used into membrane separation via mixed-matrix approach for simultaneous removal of H_2S and CO_2 from natural gas – a challenging and economically-important application [13]. The significant role of the asymmetric $[NbOF_5]^{2-}$ anion in the capture of multicomponent gases was demonstrated in the case of $Cu(dpa)_2NbOF_5$, dpa = 4, 4′-bipyridineacetylene (NbOFFIVE-2-Cu-i, i = interpenetrated, also termed as ZU-62). The exceptional efficiency of ZU-62 in relation to multicomponent removal was observed on one-step propylene purification [14]. ZU-62 with finely tuned pore aperture size and structure flexibility enables, for the first time, inverse size-sieving effect in Xe/Kr separation with record selectivity and ultrahigh Xe capacity. This not only paves a new way for the production of Xe and Kr from air, but also provides important clues for other very challenging gas separations [15]. A series of 2D MOFs with layered structures, $[Cu(4,4'\text{-dipyridylsulfone})_2(NbOF_5)]$ (termed as ZUL-200), $[Cu(4,4'\text{-dipyridylsulfoxide})_2(NbOF_5)]$ (ZUL-210), $[Cu(4,4'\text{-dipyridylsulfide})_2(NbOF_5)]$ (ZUL-220), was synthesized using $[NbOF_5]^{2-}$ and three allied organic ligands differing in the sulfur oxidation state as mixed linkers [16]. With good stability against air, water and heat, the sulfone-based 2D fluorinated MOFs demonstrate ultrahigh acetylene/ethylene (C_2H_2/C_2H_4) selectivity and record high-purity C_2H_4.

Interestingly, copper-containing samples of the considered MOFs (ZU-62, ZUL-200, ZUL-210, ZUL-220) were synthesized through the reaction of pre-prepared $CuNbOF_5$, which contained water molecules [14–17]. This compound in the form of $CuNbOF_5{\cdot}4H_2O$ was reported by Marignac as early as 1866 [18]. The compound is isostructural with $CuTiF_6{\cdot}4H_2O$, which crystallizes in the monoclinic system $P2_1/c$ and consists of chains of alternating corner sharing $[TiF_4(F)_{2/2}]^{0.5-}$ (“key”) and $[Cu(H_2O)_4(F)_{2/2}]^{0.5+}$ (“lock”) octahedra [19]. Fourquet and co-authors investigated crystal structure of $CuNbOF_5{\cdot}4H_2O$ using the bond valence sums (BVS) method, which resulted in an overall formula of $CuNb(OH)_xF_{7-x}{\cdot}3H_2O$ ($x \approx 3$) [20]. However, using the infrared spectroscopy data, Heier and Poeppelmeier confirmed the presence of the $[NbOF_5]^{2-}$ anion in this compound and concluded that disorder in the crystal structure of $CuNbOF_5{\cdot}4H_2O$ caused misleading BVS results and led to the assignment of the incorrect formula [21]. They estimated the Fourquet's crystallographic determination of the structure as careful and precise but mentioned that “even the best X-ray analysis cannot, unfortunately, differentiate between F^- and O^{2-} when disorder is present” and suggested the possible disorder mechanism in $CuNbOF_5{\cdot}4H_2O$ with one site split between bridging O^{2-} and F^- in linear chains of alternating $[NbF_4(F/O)_{2/2}]^{0.5-}$ and $[Cu(H_2O)_4(F/O)_{2/2}]^{0.5+}$ octahedra in accordance with *trans*-directing properties of $[NbOF_5]^{2-}$.

In this paper, we refine the single-crystal structure of the complex and describe it as a unique compound among all mixed metal inorganic and hybrid compounds, in which the *trans*-directing properties of $[NbOF_5]^{2-}$ are realized through a strong O–H···F hydrogen bond, which affects its thermal properties.

2. Experimental

Caution. *Hydrofluoric acid solution is highly corrosive! It must be handled with extreme caution and the appropriate protective gear and training* [22–24].

2.1. Synthesis

All the initial substances used for synthesis ($Nb_2O_5{\cdot}xH_2O$, $CuF_2{\cdot}2H_2O$, $CuCl_2{\cdot}4H_2O$, or $CuSO_4{\cdot}5H_2O$ and HFaq) were of a reagent grade (“chemically pure”). Well-shaped $CuNbOF_5{\cdot}4H_2O$ single crystals were prepared by the dissolution of hydrous niobium(V) oxide in an excess of concentrated hydrofluoric acid under heating followed by adding of stoichiometric quantities of one of the copper salts ($CuF_2{\cdot}2H_2O$, $CuCl_2{\cdot}4H_2O$ or $CuSO_4{\cdot}5H_2O$) (for example, 10.0 g of $Nb_2O_5{\cdot}xH_2O$, 25 ml of 40% HF and 10.5 g of $CuF_2{\cdot}2H_2O$ were used). The solutions were filtered and evaporated slowly in air at room temperature. The bright blue crystals of the complex of different shapes and sizes (up to 15–20 mm, Fig. 1) were recovered periodically during the crystallization process, and different portions of crystals were checked on fluorine content by distillation of H_2SiF_6 or by pyrohydrolysis at 400 °C followed by titration with $Th(NO_3)_4$. The fluorine content averaged (in mass %) 27.2 ± 0.5, which corresponded to the real composition $CuNbO(OH)_xF_{5-x}{\cdot}4H_2O$ ($x = 0.2$). Calcd. for $CuNbO(OH)_{0.2}F_{4.8}{\cdot}4H_2O$: F, 26.9. Calcd. for $CuNbOF_5{\cdot}4H_2O$: F, 28.0. The recrystallization from the HF-acidulous solution did not change the crystal composition.

2.2. X-ray studies

Powder X-ray diffraction (XRD) analysis using a D8 Advance diffractometer was carried out on the powder obtained by crushing part of a single crystal sample, which reconfirmed the pure $CuNbOF_5{\cdot}4H_2O$ phase (PDF-2 card No. 01-082-1933, Ref. 20) in full agreement with [21]. Single crystal for X-ray photography was carefully selected under a microscope and brought to the required size by partial dissolution in a water droplet. X-ray diffraction data were collected at 293 K using Bruker KAPPA APEX II diffractometer equipped with a graphite monochromator (Mo Kα radiation, λ = 0.71073 Å). Data collections were carried out with 0.3° ω-scans in hemisphere of reciprocal space with an exposure time of 20 s per frame at a crystal–detector distance of 40 mm. Data reduction and refinement were performed using the Bruker APEX2 software package [25]. All the calculations were performed with SHELXTL/PC program [26,27]. The structure was solved by direct methods with an analysis of electron density cross sections and refined against F^2 by the full-matrix least-squares method in the anisotropic approximation of non-hydrogen atoms. Hydrogen atoms of water molecules were determined from Fourier difference syntheses and refined with the use a riding model on the oxygen atoms to which they were attached using DFIX options. Structural information is presented in Table 1, the selected distances and angles are shown in Table 2, and Table 3 gives the parameters of hydrogen bonds.

2.3. Infrared spectroscopy

The room temperature infrared (250–4000 cm^{-1}) spectra of $CuNbOF_5{\cdot}4H_2O$ were collected in Nujol mull using a Shimadzu FTIR Prestige-21 spectrometer operating at a 2 cm^{-1} resolution. The KBr, CsI or CaF_2 plates were used as underlayers. The samples run as KBr pellets resulted

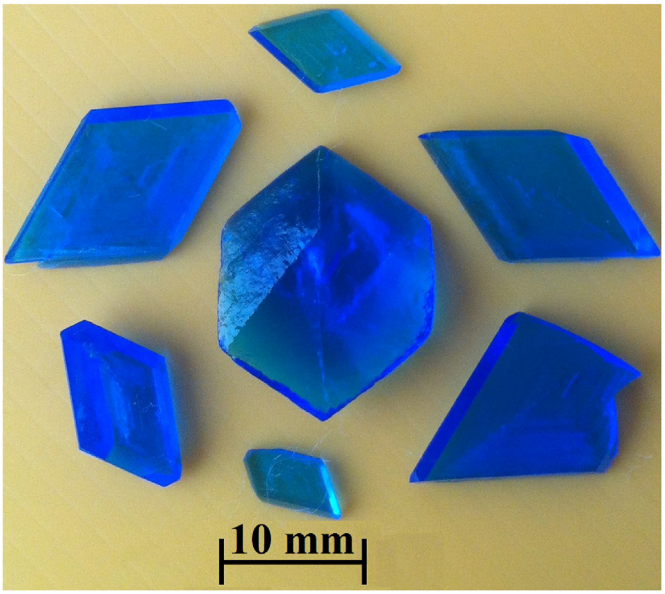

Fig. 1. Single crystals of $CuNbOF_5{\cdot}4H_2O$.

Table 1
Crystal and experimental data for $CuNbOF_5{\cdot}4H_2O$.

CCDC Code	2149514
Chemical formula	$Cu(H_2O)_4NbOF_5$
M_r	341.01
Temperature (K)	293(2)
Crystal system, space group	Monoclinic, $P2_1/c$
a (Å) b (Å) c (Å)	5.5830(1), 9.9641(2), 7.5293(1)
β (deg)	103.359(1)
V (Å^3)	407.52(1)
Z	2
D_x (Mg m^{-3})	2.779
Radiation type	Mo $K\alpha$
μ [mm^{-1}]	4.075
Crystal size (mm)	0.18 × 0.18 × 0.18
Data collection	
Diffractometer	Bruker KAPPA APEX-II
Absorption	Multi-scan *SADABS*
No. of measured, independent and observed [I > 2σ(I)] reflections	11179, 2999, 2376
R_{int}	0.0227
θ_{max} (°)	43.026
Refinement	
R [$F^2 > 2\sigma(F^2)$], $wR(F^2)$, S	0.0241, 0.0668, 0.987
No. of reflections	2376
No. of parameters	74
$\Delta\rho_{max}$, $\Delta\rho_{min}$ (e Å^{-3})	0.509, −1.081

Table 2
Selected distances (Å) and angles (°) for $CuNbOF_5{\cdot}4H_2O$.

Nb1–F1	1.943(2)	O3–F1	2.705(1) × 2
Nb1–F1A	1.888(2)	O3–F2	2.724(1) × 2
Nb1–F2	1.955(2)	O3–F1A	2.727(1) × 2
Nb1–F2A	1.929(2)	O3–F2A	2.746(1) × 2
Nb1–O3	1.815(1)	F1–F2	2.702(1) × 2
Nb1–F3A	2.043(1)	F2–F1A	2.744(1) × 2
O3–Nb1–F1	92.01(7)	F1–Nb1–F2	87.77(7)
O3–Nb1–F2	92.45(7)	F2–Nb1–F1A	91.08(8)
O3–Nb1–F1A	94.84(6)	F1A–Nb1–F2A	90.11(7)
O3–Nb1–F2A	94.28(6)	F2A–Nb1–F1	90.23(8)
O3A–Nb1–F1	86.30(5)	O3–Nb1–O3A	178.13(9)
O3A–Nb1–F2	86.70(5)	F1–Nb1–F1A	173.10(5)
O3A–Nb1–F1A	86.84(7)	F2–Nb1–F2A	173.05(4)
O3A–Nb1–F2A	86.52(6)		
Cu1–O1	1.961(1) × 2	O1–O2	2.717(1) × 2
Cu1–O2	1.957(1) × 2	O1–O2A	2.823(1) × 2
Cu1–F1	2.295(1) × 2	F1–O2	2.955(1) × 2
O1–F1	3.048(1) × 2	F1–O2A	3.077(1) × 2
O1–F1B	2.989(1) × 2	F1–Cu1–O2	87.64(4) × 2
O1–Cu1–F1	91.14(4) × 2	O2–Cu1–F1B	92.36(4) × 2
O1–Cu1–O2	87.81(3) × 2	O1–Cu1–O1A	180
O1–Cu1–F1B	88.86(5) × 2	O2–Cu1–O2A	180
O1–Cu1–O2A	92.19(3) × 2	F1–Cu1–F1A	180

in substantial changes in the spectrum due to interaction of the complex with KBr.

2.4. Thermogravimetric analysis (TG-DTA-DTG)

Thermogravimetric measurements for $CuNbOF_5{\cdot}4H_2O$ were performed with a Netzsch STA 449C. The samples (about 10 mg) were placed in Pt crucible with pierced lid and heated in 20–300 °C at a rate of 5 deg/min under an argon atmosphere. Furthermore, the thermal decomposition of the compound under quasi-isobaric conditions (in conic Pt-labyrinth crucible) was carried out with the Derivatograph Q-1500D (MOM, Budapest). Special form of crucible ensures a constant partial pressure (about 70 kPa) of the gaseous reaction products, which can be described as 'self-generated' atmosphere or conditions as non-reciprocal quasi-isobaric [28]. Such conditions allow the single steps of thermal decomposition to be better separated. The sample mass of 200–400 mg was heated at a dynamic heating rate of 5 deg/min up to 300 °C at ambient conditions. The initial substances, intermediates and final products of the decomposition reactions were characterized by X-ray powder analysis (diffractometer D8 Advance, CuK_α-radiation), infrared spectroscopy and chemical analysis for fluorine content.

Table 3
Hydrogen bonds geometry (Å, °) in the $CuNbOF_5{\cdot}4H_2O$ structure.

D –H···*A*	*D*–H	H···A	*D*···*A*	*D*–H···A
O1–H1···X3^{i} *	0.970	1.793	2.754(1)	170
O1–H2···X3^{ii}	0.972	1.723	2.682(1)	169
O2–H3···F2^{iii}	0.969	1.742	2.707(1)	173
O2–H4···F2^{iv}	0.965	1.774	2.732(1)	171

Symmetry codes: (i) $x, -y+1/2, z-½$; (ii) $x, y, z-1$; (iii) $x-1, -y+1/2, z-1/12$; (iv) $x-1, y, z$. *X = F(O).

3. Results and discussion

3.1. Crystal structure

It should be noted that the modification of synthetic method of $CuNbOF_5{\cdot}4H_2O$ concerning mainly the starting copper compound ($CuF_2{\cdot}2H_2O$, $CuCl_2{\cdot}4H_2O$ or $CuSO_4{\cdot}5H_2O$) instead of CuO [20,21] or $CuCO_3$ [29] did not lead to any change in the composition of the final product (according to X-ray powder data), but ensured the growth of higher quality single crystals. The fluorine content was also the same in all cases. Here we use the stoichiometric formula $CuNbOF_5{\cdot}4H_2O$, since X-ray diffraction is not sensible to the hydroxide impurity in the compound composition.

At the first stage of structural determination by the direct method, heavy Nb and Cu atoms in special positions and light (X = F, O) atoms in general positions were unambiguously determined. Light atoms in the Cu environment were taken as O atoms, and in the Nb environment, as F atoms. The next step was to refine the structure with these atoms in the anisotropic approximation to $R_1 = 0.0303$. Four peaks of electron density with a height of 0.75–0.64 e Å^{-3}, which corresponded to the hydrogen atoms of water molecules (O–H 0.79 and 0.86 Å, and H–O–H = 106 and 109°), were clearly manifested in the difference electron density near oxygen atoms. Refinement of the structure with hydrogen atoms reduced R_1 to 0.0282. To balance the valences of the cation and anion, the cross section of the electron density of the Nb atom was constructed (Fig. 2). It is seen that the Nb atom in the structure is not located at the center of symmetry (2*d*). It is split and occupies the general position (4*e*). Refinement of the structure with a displaced Nb atom lowered R_1 to 0.0245. The displacement of the atom from the center of symmetry by 0.118(1) Å led to two distances Nb–F3 1.815(1) and 2.043(1) Å, which correspond to Nb–O and Nb–F bonds, respectively (Table 2). Refinement of the structure with an average F and O atomic scattering curve for the F3 atom lowered R_1 to 0.0241, while refinement of the structure with the replacement of the bridging F1 atom by an O atom increased R_1 to 0.0285. Therefore, bridging atoms in the polymer chain – Nb–X–Cu–X–Nb – are fluorine atoms, and the position of the F3 atom is statistically occupied by F and O atoms. Thus, monoclinic structure of the complex consists of bent chains of *trans-F*-linked alternate $[Cu(H_2O)_4(F)_{2/2}]^+$ and $[Nb(O/F)_2F_2(F)_{2/2}]^-$ octahedra, running along the [101] direction (Fig. 3).

In the related $MnNbOF_5{\cdot}4H_2O$ complex (only one purely inorganic compound among the structurally characterized mixed metal compounds based on $[NbOF_5]^{2-}$ in the CCDC database, Table S1), the bridging atoms between two octahedra are the O and F (*trans* to O) atoms [30]. This structure was also refined with splitting the average position of the Nb atom in the disordered anion into discrete quasi-isotropic atomic positions. Such a procedure was originally applied by Stomberg for

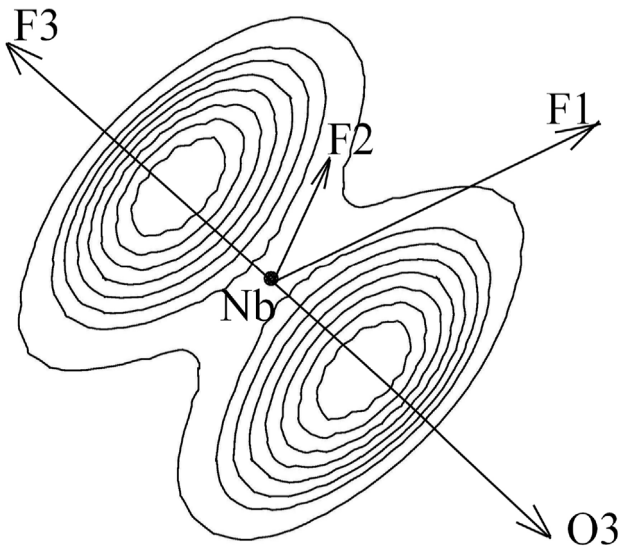

Fig. 2. Electron density distribution of Nb in $CuNbOF_5{\cdot}4H_2O$ on the (010) plane at $b = 0$.

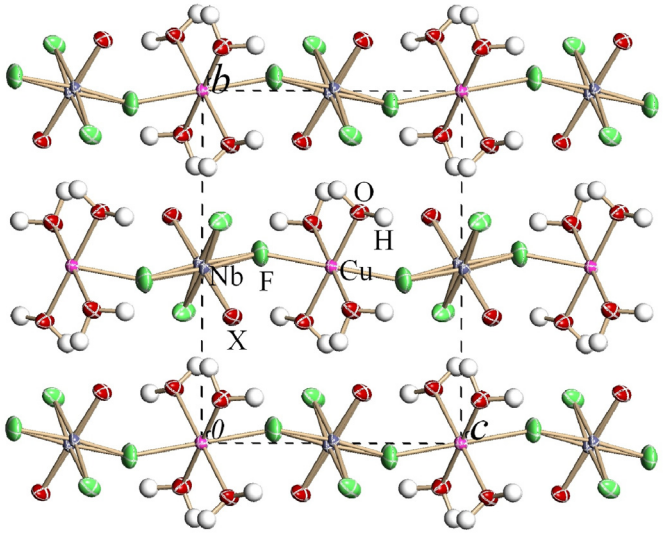

Fig. 4. Crystal structure of $CuNbOF_5{\cdot}4H_2O$. View along the *a*–axis.

disordered Na_2NbOF_5 [31].

The crystal structure of $CuNbOF_5{\cdot}4H_2O$ is layered (Fig. 4). The layers are formed from polymer chains elongated along the [1 0 1] axis, which are interconnected by hydrogen bonds O–H···F (O···F = 2.682–2.754 Å) into layers parallel to the (0 1 0) plane. These layers are linked to each other into a framework also by relatively short hydrogen bonds O2–H3···F2 (O···F = 2.707 Å) (Table 3). In the structure, each $NbOF_5$ polyhedron is hydrogen bonded to six $Cu(H_2O)_4F_2$ polyhedra and vice versa (Fig. 5). Hydrogen bonds in $CuNbOF_5{\cdot}4H_2O$ (O···F 2.682–2.754 Å) are noticeably shorter than those in α–$MnNbOF_5{\cdot}4H_2O$ (2.759–2.801 Å). The strongest hydrogen bond is precisely formed by disordered O and F ligands with water molecules (2.682 Å), so that the *trans*-directing properties of the $[NbOF_5]^{2-}$ anion are realized through this strong hydrogen bond, and not through a conventional bridge $(O/F)_{2/2}$ bond with LTM (Cu), in difference with Mn. Only in two cases (see Table S1) it was reported that niobium was joint to LTM via the F bridge, which raises certain doubts, since the Nb–O and Nb–F distances in the structures of presented compounds differ slightly [32,33]. These are $[Cu(pyz)]_2NbOF_5$, pyz = pyrazine [32], and $CoNbOF_5(pyz)(H_2O)_2$ [33]. The disordered crystal structure of the latter was also reported by Hu et al. where alternating CoN_2O_3F and $NbOF_5$ octahedra are sharing corner-O/F atoms with the Nb–(O,F) bond of 1.930(2) Å [34], while Zhou et al. assume that F2/O2 is equally disordered in the equatorial plane, because of strong hydrogen bonding [33]. However, according to Poeppelmeier et al., hydrogen bonding is one of the strategies to order the O^{2-}/F^- anions [35]. Very few crystal structures were determined with orientational disorder when the anions are isolated into hydrogen bond networks. Two features responsible for the O^{2-}/F^- ordering: the high coordination number of each O^{2-}/F^- ligand with hydrogen atoms and the flexibility of the hydrogen bonding [35]. We refined the structure of $CoNbOF_5(pyz)(H_2O)_2$ according to the experimental data available (CCDC 2024754) [33]. The Nb ellipsoid is extended in the direction of the bridging atoms, in contrast to the Nb ellipsoid in our $CuNbOF_5{\cdot}4H_2O$ structure (Fig. 6). The shape of the ellipsoids indicates that the Nb atoms in the two structures are displaced from the symmetry center, but in different directions. In the process of structure refinement of $CoNbOF_5(pyz)(H_2O)_2$ with a displaced Nb atom, its coordinates became (0.492 0.5 0.978), and the Nb–X1 distances were 1.791 and 2.055 Å, which correspond to the Nb–O and Nb–F bond lengths, respectively. The R_1 with the split Nb and disordered F1 and O1 atoms decreased from 0.0417 to 0.0376. Therefore, the bridging atoms in the $CoNbOF_5(pyz)(H_2O)_2$ structure are the F and O atoms. HBs of different strength of the O–H···F and O–H···O types are reflected in the IR spectra of the complex and affect its thermal behavior.

3.2. Infrared spectra and thermal properties

The infrared spectrum of $CuNbOF_5{\cdot}4H_2O$ is shown in Fig. 7. The strong intensive band at 910 cm^{-1} is assigned to the ν(Nb–O) stretch in accordance with the short distance of this bond, 1.815(1) Å, and its triple character ($\sigma + 2\pi$) [36,37]. This wavenumber is close to those reported for a series of mixed metal $NbOF_5$-based compounds (Table S1), which lie in the region 890–925 cm^{-1}. The significant difference between the reported stretching vibrations ν(Nb–O) (917 cm^{-1}) [29] and (972 cm^{-1}) [21] in the case of $CuNbOF_5{\cdot}4H_2O$ can be explained by different

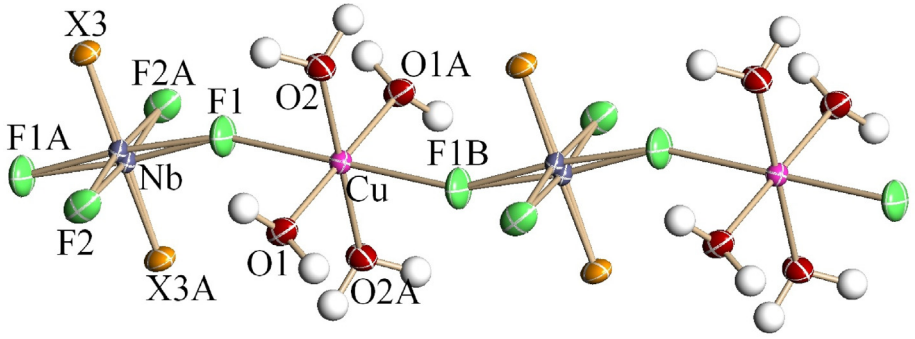

Fig. 3. The structure of the infinite bent chain in $CuNbOF_5{\cdot}4H_2O$.

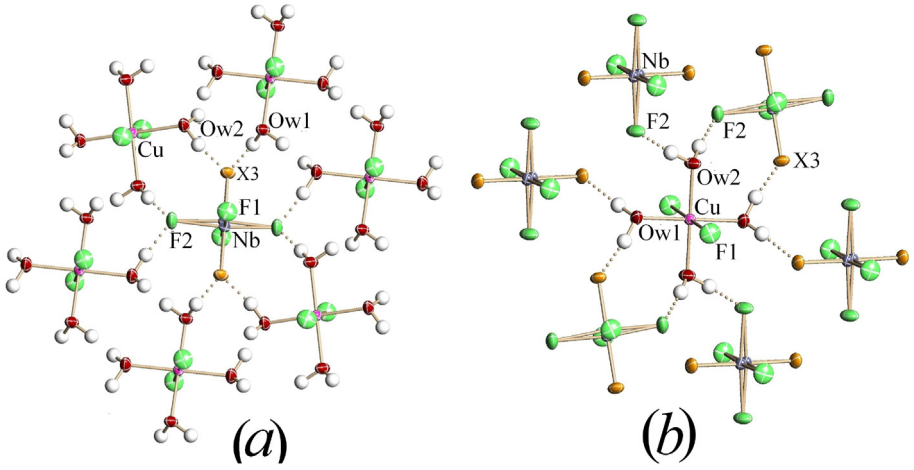

Fig. 5. Fragments of the structure with hydrogen bonds around Nb (a) and Cu (b) octahedra.

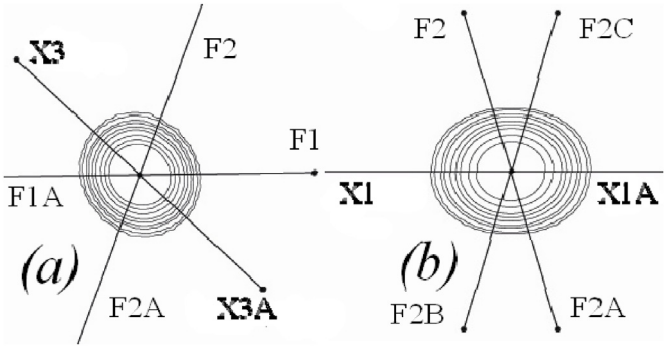

Fig. 6. Electron density distribution of Nb in $CuNbOF_5{\cdot}4H_2O$ (*a*) and $CoNbOF_5(pyz)(H_2O)_2$ (*b*) on the (100) plane at $a = 0.5$.

conditions for recording the IR spectrum.

The point is that in the latter case the substance reacted with KBr. Similar interaction was well pronounced when CsJ was used. The brown coloring of the mixture was observed due to the following possible reaction:

$$CuNbOF_5{\cdot}4H_2O + 2CsI = CsCuNbOF_4I{\cdot}4H_2O + 0.5I_2 + CsF$$

It is clear that replacement of *trans*-fluoride by iodide results in the frequency increase of the ν(Nb–O) stretch (to 970–974 cm^{-1}). The DFT (density functional theory, B3LYP, 3-21G) calculations of uncoordinated $[NbOF_5]^{2-}$ (C_{4v}) show the appearance ν(Nb–O) at 921 cm^{-1} and ν(Nb–F_{trans}) at 487 cm^{-1}. The bending δ(Nb–O, F) vibrations lie at about 300 cm^{-1} and lower, so the band at 469 cm^{-1} (Fig. 7) can be assigned to ν(Nb–F_{trans}) while ν(Nb–F_{eq}) appear at 500–600 cm^{-1} (peak at 570 cm^{-1}). Two ν(Nb–F_{trans}) bands at 410 and 399 cm^{-1} were previously reported for Rb_2NbOF_5 [38]. The band at 380 cm^{-1} can be probably assigned to ν(Cu–F) or/and to (Cu–Ow) stretches. Absorption bands at 3425 cm^{-1} and 1660-1650 cm^{-1} are assigned to stretching and bending vibrations of water molecules, respectively. The strong hydrogen bonds appear in the spectrum as a broad band at 3000–3300 (peak at 3184) cm^{-1} assigned to ν(OH) stretches. Moreover, a broad shoulder at 700–800 (peak at 768) cm^{-1} might be attributed, we assume, to transverse vibration of a proton in a ternary system O–H···F with strong HB (O···F distance of 2.682 Å). There is no such strong hydrogen bond in $MnNbOF_5{\cdot}4H_2O$, which dehydrates in two stages to form anhydrous $MnNbOF_5$ [30]. A completely different picture is observed in the case of $CuNbOF_5{\cdot}4H_2O$.

Fig. 8a shows the thermal behavior of $CuNbOF_5{\cdot}4H_2O$ under quasi-isobaric conditions (labyrinth crucible). Attention is drawn to the presence of an endothermic effect at 88 °C with virtually no loss of mass, which indicates a phase transition (PT) that is absent under open crucible conditions (Fig. 8b) and under the conditions of a Pt crucible with a pierced lid in an argon atmosphere (Fig. S1).

We checked the presence of possible temperature PTs in this compound by X-ray diffraction. When the temperature is lowered to 173 K, the crystal structure is completely preserved, and when heated above 325 K, the single crystal begins to pass into a polycrystalline state (diffraction rings appear on the monitor). At 330 K, the crystal completely and irreversibly passes into the polycrystalline state within 30 min, which makes it impossible to determine the structure of the new phase. However, this new phase appeared in the IR spectrum of the compound (see insert in Fig. 7) as a new ν(Nb–O) stretching vibration at 955 cm^{-1} after the spectrum of the sample heated to 100 °C was immediately recorded. This means the weakening of strong O–H···F HBs and formation of ordinary chains of alternating Cu and Nb octahedra through *trans*-(O, F) bridges.

Further heating resulted in three-step thermal decomposition of $CuNbOF_5{\cdot}4H_2O$ (Fig. 8). In accordance with the mass loss and fluorine content, two first stages are connected with the sequential evolution of two water molecules at 125 and 177 °C in labirinth crucible and at 90 and 165 °C in open crucible. The third stage at 263 (261) °C simultaneously includes the pyrohydrolysis and dehydration processes. The idealized decomposition scheme can be expressed as follows:

$CuNbOF_5{\cdot}4H_2O \rightarrow CuNbOF_5{\cdot}3H_2O + H_2O$, $CuNbOF_5{\cdot}3H_2O \rightarrow CuNbOF_5{\cdot}2H_2O + H_2O$ (Δm = 6.2 (5.2)%, calculated 5.3%); $CuNbOF_5{\cdot}2H_2O \rightarrow CuNbO_2F_3 + 2HF + H_2O$ (Δm = 15.6 (14.5)%, calculated 17.1%)

Noticeably, under quasi-isobaric conditions, the process of pyrohydrolysis proceeds somewhat deeper. The total mass loss of 28.6 (25.2) % (average 26.9%) is close to the theoretical one in accordance with the evolution of ($3H_2O$ + 2HF) (27.7%). The X-ray powder pattern of the final product $CuNbO_2F_3$ corresponds mainly to cubic phase of the ReO_3 type. It should be noted that pyrohydrolysis accompanies the thermal degradation of piperazine complex of niobium $(C_4H_{12}N_2)NbOF_5$ with the evolution of one $C_4H_{10}N_2$ and two HF molecules per formula unit [39]. The end-product of thermal decomposition of $Cu(H_2O)_2(pyz)NbOF_5$ at 600 °C was analyzed to contain NbO_2F (ReO_3 type) [34].

4. Conclusions

To date, $CuNbOF_5{\cdot}4H_2O$ is the only case among mixed metal oxyfluoroniobates when the *trans*-directing properties of the anion manifest themselves through the formation of a strong O–H···F hydrogen bond, and not through the alignment of the ordinary linear chain of alternating metal-niobium octahedra, connected by conventional O/F bridges.

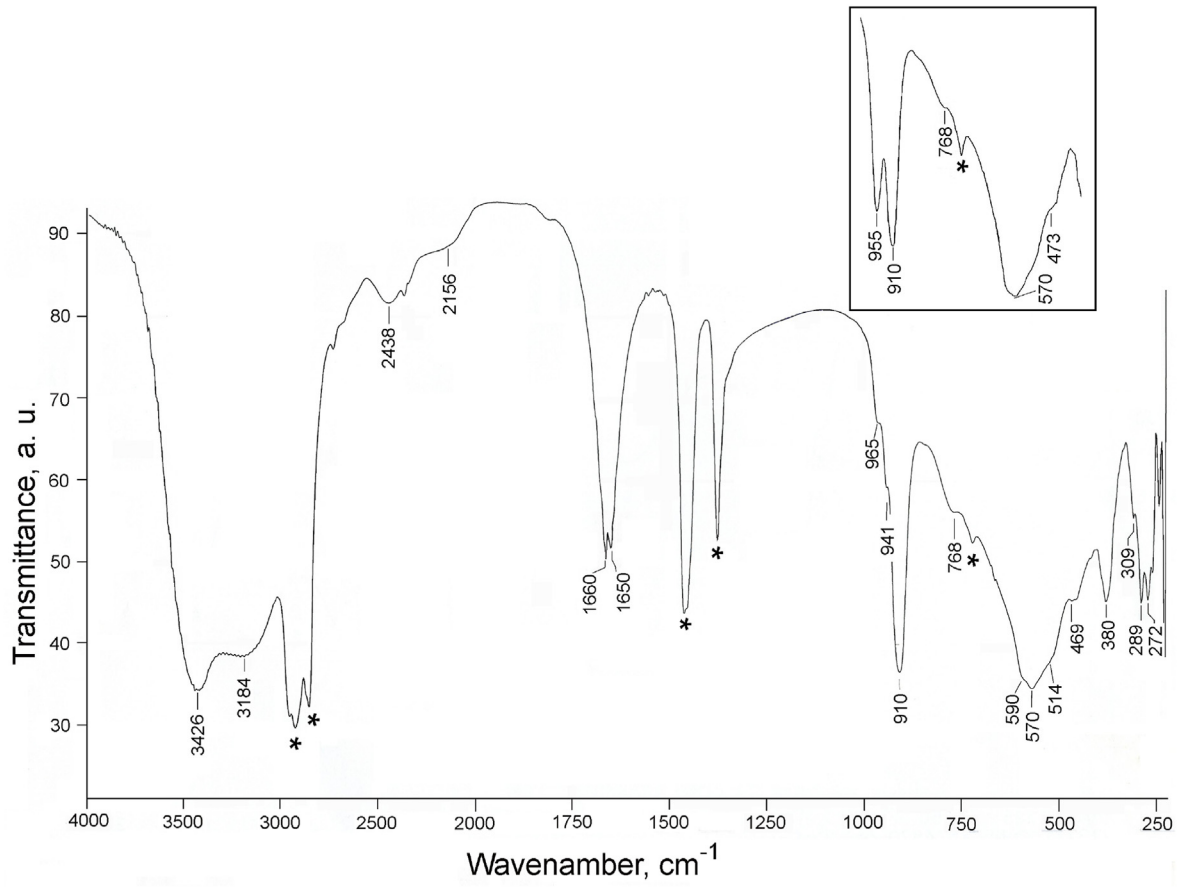

Fig. 7. Room temperature IR spectrum of $CuNbOF_5 \cdot 4H_2O$. Insert - IR spectrum of the complex taken immediately after the phase transition at 88 °C. *– bands of Nujol mull.

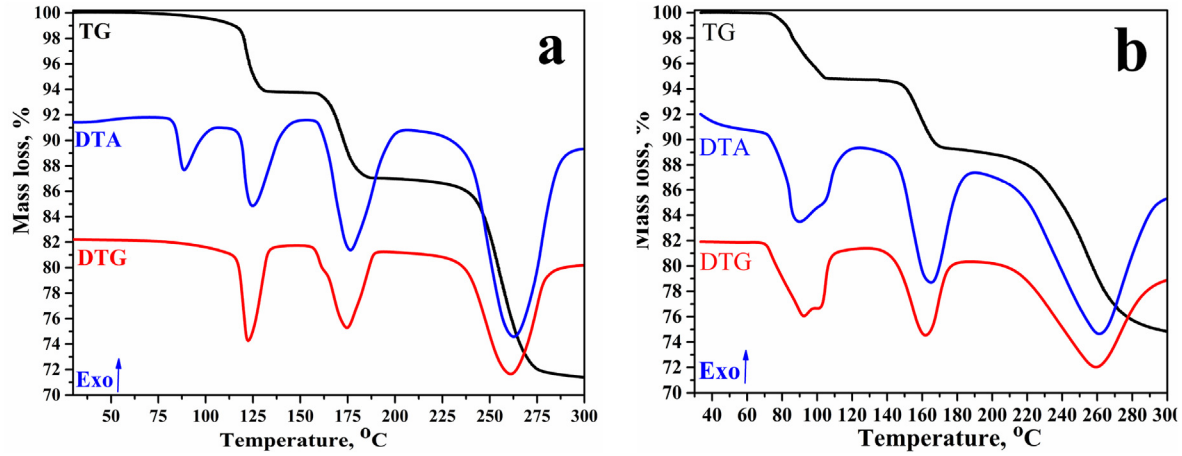

Fig. 8. Thermal curves of $CuNbOF_5 \cdot 4H_2O$ in quasi-isibaric conditions in labirinth crucible (a) and in open crucible (b).

Refinement of the crystal structure of the complex by X-ray diffraction with the splitting of the niobium atom over two positions revealed the real geometry of the anion in the disordered structure and confirmed its composition ($CuNbOF_5 \cdot 4H_2O$) described by Marignac as early as 1866. We observed for the first time a phase transition at 88 °C under quasi-isobaric conditions, associated with the rearrangement of hydrogen bonds and a change in the *trans*-directing properties of $[NbOF_5]^{2-}$. The presence of strong hydrogen bonds O–H···F is responsible for the occurrence of pyrohydrolysis processes in this compound, so that the preparation of anhydrous $CuNbOF_5$ is rather problematic, as is the unreliable indication of the existence of hexahydrated $CuNbOF_5 \cdot 6H_2O$ (to prepare microcrystalline NbOFFIVE-3-Cu) [40], which will not be described by the "lock and key" model.

CRediT authorship contribution statement

N.M. Laptash: Conceptualization, Investigation, Writing – original draft, Writing – review & editing. **A.A. Udovenko:** Investigation, Writing – review & editing. **A.D. Vasiliev:** Investigation, Writing – review & editing. **E.B. Merkulov:** Investigation.

Declaration of competing interest

The authors declare that they have no known competing financial interests or personal relationships that could have appeared to influence the work reported in this paper.

Data availability

Data will be made available on request.

Acknowledgments

We thank Dr. T.B. Emelina for the DFT calculations of uncoordinated $[NbOF_5]^{2-}$ anion. The work was partially supported within the frames of the State Order of the Institute of Chemistry, Far Eastern Branch of the Russian Academy of Sciences (project No. FWFN 0205–2022–0003).

Appendix A. Supplementary data

Supplementary data to this article can be found online at https://doi.org/10.1016/j.jssc.2022.123781.

References

[1] R. Gautier, K.R. Poeppelmeier, Alignment of acentric units in infinite chains: a "lock and key" model, Cryst. Growth Des. 13 (2013) 4084–4091.
[2] M.E. Welk, A.J. Norquist, F.P. Arnold, C.L. Stern, K.R. Poeppelmeier, Out-of-center distortions in d^0 transition metal oxide fluoride anions, Inorg. Chem. 41 (2002) 5119–5125.
[3] H.K. Izumi, J.E. Kirsch, C.L. Stern, K.R. Poeppelmeier, Examining the out-of-center distortion in the $[NbOF_5]^{2-}$ anion, Inorg. Chem. 44 (2005) 884–895.
[4] P.A. Maggard, A.L. Kopf, C.L. Stern, K.R. Poeppelmeier, Probing helix formation in chains of vertex-linked octahedral, CrystEngComm 6 (2004) 451–457.
[5] J.T. Li, P.M. Bhatt, J.Y. Li, M. Eddaoudi, Y.L. Liu, Recent progress on microfine design of metal-organic frameworks: structure regulation and gas sorption and separation, Adv. Mater. 32 (2020), 2002563.
[6] L.F. Yang, S.H. Qian, X.B. Wang, X.L. Cui, B.L. Chen, H.B. Xing, Energy-efficient separation alternatives: metal-organic frameworks and membranes for hydrocarbon separation, Chem. Soc. Rev. 49 (2020) 5359–5406.
[7] W.D. Fan, X.R. Zhang, Z.X. Kang, X.P. Liu, D.F. Sun, Isoreticular chemistry within metal-organic frameworks for gas storage and separation, Coord. Chem. Rev. 440 (2021), 213968.
[8] X.F. Li, H. Bian, W.Q. Huang, B.Y. Yan, X.Y. Wang, B. Zhu, A review on anion-pillared metal organic framework (APMOF) and its composites with the balance of adsorption capacity and separation selectivity for efficient gas separation, Available at SSRN, https://ssrn.com/abstract=4076661, 2022, https://doi.org/10.2139/ssrn.4076661.
[9] A. Cadiau, K. Adil, P. Bhatt, Y. Belmabkhout, M. Eddaoudi, A metal-organic framework-based splitter for separating propylene from propane, Science 353 (2016) 137–140.
[10] D. Antypov, A. Shkurenko, P.M. Bhatt, Y. Belmabkhout, K. Adil, A. Cadiau, M. Suetin, M. Eddaoudi, M.J. Rosseinsky, M.S. Dyer, Differential guest location by host dynamics enhances propylene/propane separation in a metalorganic framework, Nat. Commun. 11 (2020) 6099.
[11] P.M. Bhatt, Y. Belmabkhout, A. Cadiau, K. Adil, O. Shekhah, A. Shkurenko, L.J. Barbour, M. Eddaoudi, A fine-tuned fluorinated MOF addresses the needs for trace CO_2 removal and air capture using physisorption, J. Am. Chem. Soc. 138 (2016) 9301–9307.
[12] J.Y. Lv, Y.W. Cui, J.H. Yang, L.G. Li, X.R. Zhou, J.M. Lu, G.H. He, Inorganic pillar center-facilitated counter-diffusion synthesis for highly H_2 perm-selective KAUST-7 membranes, ACS Appl. Mater. Interfaces 14 (2022) 4297–4306.
[13] G. Liu, A. Cadiau, Y. Liu, K. Adil, V. Chernikova, I.D. Carja, Y. Belmabkhout, M. Karunakaran, O. Shekhah, C. Zhang, A.K. Itta, S.L. Yi, M. Eddaoudi, W.J. Koros, Enabling fluorinated MOF-based membranes for simultaneous removal of H_2S and CO_2 from natural gas, Angew. Chem. Int. Ed. 57 (2018) 14811–14816.
[14] L. Yang, X. Cui, Z. Zhang, Q. Yang, Z. Bao, Q. Ren, H. Xing, Asymmetric anion-pillared metal-organic framework as multisite-adsorbent enables simultaneous removal of propyne and propadiene from propylene, Angew. Chem. Int. Ed. 57 (2018) 13145–13149.
[15] Q.J. Wang, T. Ke, L.F. Yang, Z.Q. Zhang, X.L. Cui, Z.B. Bao, Q.L. Ren, Q.W. Yang, H.B. Xing, Separation of Xe from Kr with record selectivity and productivity in anion-pillared ultramicroporous materials by inverse sizesieving effect, Angew. Chem. Int. Ed. 59 (2020) 3423–3428.
[16] J. Shen, X. He, T. Ke, R. Krishna, J.M. van Baten, R.D. Chen, Z.B. Bao, H.B. Xing, M. Dinc, Z.G. Zhang, Q.W. Yang, Q.L. Ren, Simultaneous interlayer and intralayer space control in two-dimensional metal-organic frameworks for acetylene/ethylene separation, Nat. Commun. 11 (2020) 6259.
[17] L. He, J.K. Natha, Q. Lin, Robust multivariate metal-porphyrin frameworks for efficient ambient fixation of CO_2 to cyclic carbonates, Chem. Commun. 55 (2019) 412–415.
[18] M.C. Marignac, Les combinaisons du Niobium, Ann. Chem. Phys. 8 (1886) 5–75.
[19] J. Fischer, G. Keib, R. Weiss, Structure cristalline du fluorotitanate de cuivre tétrahydraté, $CuTiF_6{\cdot}4H_2O$, Acta Crystallogr. 22 (1967) 338–340.
[20] M.P. Crosnier-Lopez, H. Duroy, J.L. Fourquet, About the crystal structure of $CuNb(OH, F)_7{\cdot}3H_2O$, J. Solid State Chem. 108 (1994) 398–401.
[21] K.R. Heier, K.R. Poeppelmeier, Reinvestigation of $CuNbOF_5{\cdot}4H_2O$, J. Solid State Chem. 133 (1997) 576–579.
[22] J.C. Bertolini, Hydrofluoric acid: a review of toxicity, J. Emerg. Med. 10 (1991) 163–168.
[23] D. Peters, R. Miethchen, Symptoms and treatment of hydrogen fluoride injuries, J. Fluorine Chem. 79 (1996) 161–165.
[24] E.B. Segal, First aid for a unique acid, HF: a sequel, Chem. Health Saf. 7 (2000) 18–23.
[25] APEX2, Bruker AXS Inc., Madison, WI, 2012.
[26] G.M. Sheldrick, SHELXT – integrated space-group and crystal-structure determination, Acta Crystallogr. A: Found. Adv. 71 (2015) 3–8.
[27] G.M. Sheldrick, Crystal structure refinement with SHELXL, Acta Crystallogr. C: Struct. Chem. 71 (2015) 3–8.
[28] D.H. Menz, The characterization of the thermal behaviour of inorganic fluorides using quasi-static thermoanalytical methods, J. Therm. Anal. 38 (1992) 321–334.
[29] R.L. Davidovich, T.F. Levchishina, T.A. Kaidalova, V.I. Sergienko, The synthesis and properties of oxofluoroniobates and fluorotantalates of bivalent metals, J. Less Common. Met. 27 (1972) 35–43.
[30] A.V. Gerasimenko, I.A. Tkachenko, E.B. Merkulov, T.F. Antokhina, Crystal structures of $MnNbOF_5{\cdot}4H_2O$ at 153 and 297 K, Russ. J. Inorg. Chem. 55 (2010) 1888–1896.
[31] R. Stomberg, The crystal structure of sodium pentafluorooxoniobate(2–), $Na_2[NbF_5O]$, Acta Chem. Scand. A: Phys. Inorg. Chem. 38 (1984) 603–607.
[32] H. Lin, P.A. Maggard, Microporosity, optical bandgap sizes, and photocatalytic activity of M(I)–Nb(V) (M = Cu, Ag) oxyfluoride hybrids, Cryst. Growth Des. 10 (2010) 1323–1331.
[33] Y.D. Zhou, Y.D. Wang, J.J. Cao, Z. Zeng, T.P. Zhou, R.G. Liao, T. Wang, Z.X. Wang, Z.C. Xia, Z.W. Ouyang, H.C. Lu, $CoMOF_5(pyrazine)(H_2O)_2$ (M = Nb, Ta): two-layered cobalt oxyfluoride antiferromagnets with spin flop transitions, Inorg. Chem. 60 (2021) 13309–13319.
[34] B. Hu, J.R. Li, X.Y. Huang, Synthesis, crystal structure, and properties of inorganic-organic hybrid M(II)-Nb(V) (M = Co, Cu) oxyfluorides, Chin. J. Struct. Chem. 30 (2011) 678–684.
[35] R. Gautier, R. Gautier, K.B. Chang, K.R. Poeppelmeier, On the origin of the differences in structure directing properties of polar metal oxyfluoride $[MO_xF_{6-x}]^{2-}$ (x = 1, 2) building units, Inorg. Chem. 54 (2015) 1712–1719.
[36] J.M. Mayer, Metal-oxygen multiple bond lengths: a statistical study, Inorg. Chem. 27 (1988) 3899–3903.
[37] N.M. Laptash, A.A. Udovenko, T.B. Emelina, Dynamic orientation disorder in rubidium fluorotantalate. Synchronous Ta-O and Ta-F vibrations, J. Fluorine Chem. 132 (2011) 1152–1158.
[38] L. Surendra, D.N. Sathyanarayana, G.V. Jere, Vibrational assignment and normal coordinate analysis of $[MOF_5]^{2-}$ (M = Nb, Ta) in the modified Urey-Bradley force field, J. Fluorine Chem. 23 (1983) 115–122.
[39] Y.Q. Feng, Z.H. Meng, Q.Z. Huang, D.F. Qiu, H.Z. Shi, Hydrothermal syntheses, crystal structures and characterizations of two new metal-fluorides based on niobium and tantalum, Inorg. Chem. Commun. 13 (2010) 1118–1121.
[40] N. Kumar, S. Mukherjee, N.C. Harvey-Reid, A.A. Bezrukov, K. Tan, V. Martins, M. Vandichel, T. Pham, L.M. van Wyk, K. Oyekan, A. Kumar, K.A. Forrest, K.M. Patil, L.J. Barbour, B. Space, Y. Huang, P.E. Kruger, M.J. Zaworotko, Breaking the trade-off between selectivity and adsorption capacity for gas separation, Chem 7 (2021) 3085–3098.